Analysis of the possible geometries of a disappeared Parthian adobe dome: from in-situ tests to finite element macro-modelling

Analysis of the possible geometries of a disappeared Parthian adobe dome: from in-situ tests to finite element macro-modelling

Daniele Ferretti* and Eva Coïsson

Department of Engineering and Architecture,
University of Parma,
Parco Area delle Scienze 181/A, 43124 Parma, Italy
Email: daniele.ferretti@unipr.it
Email: eva.coisson@unipr.it
*Corresponding author

Erica Lenticchia

Department of Structural, Geotechnical and Building Engineering,
Politecnico di Torino,
Corso Duca degli Abruzzi 24, 10129 Torino, Italy
Email: erica.lenticchia@polito.it

Elena Michelini

Department of Engineering and Architecture,
University of Parma,
Parco Area delle Scienze 181/A, 43124 Parma, Italy
Email: elena.michelini@unipr.it

Abstract: The work studies – from a structural point of view – the possible geometries of the adobe dome covering the Round Hall building in the archaeological site of Old Nisa (Turkmenistan). Thirteen dome geometries are identified, starting from archaeological reconstructions of the disappeared dome. The dome reconstructions are subsequently modelled through nonlinear finite element analysis in order to check their static behaviour. Concrete damage plasticity model is used to describe the nonlinear behaviour of adobe masonry. To calibrate the material model, the results of an onsite experimental program characterising adobe bricks are used. The analyses show that all the 13 geometries are stable with large safety margins. The results do not allow excluding some geometries, but on the contrary, highlight that the choice of the geometry of the dome was not a critical element. This aspect supports the hypothesis that the round room was actually covered by a dome.

Keywords: adobe; domes; archaeological heritage; Turkmenistan; concrete damage plasticity; FE modelling.

Reference to this paper should be made as follows: Ferretti, D., Coïsson, E., Lenticchia, E. and Michelini, E. (xxxx) 'Analysis of the possible geometries of a disappeared Parthian adobe dome: from in-situ tests to finite element macro-modelling', *Int. J. Masonry Research and Innovation*, Vol. X, No. Y, pp.xxx–xxx.

Biographical notes: Daniele Ferretti is an Associate Professor of Structural Design at the University of Parma since 2004. He is an author of 100 scientific papers on reinforced concrete structures (cracking, nonlinear analysis, FRP, FRCM), masonry (AAC, adobe) and structural/seismic behaviour of ancient buildings. He is a principal investigator of several research projects funded by firms or public administrations for the analysis of RC or masonry structures and for the seismic assessment of ancient buildings (towers, theatres, cathedrals).

Eva Coïsson is a Full Professor in Architectural Restoration at the University of Parma. Her research, carried out also guiding research projects funded by private companies or public administrations, is mainly focused on the diagnosis and analysis of the stability of ancient structures, aimed at their conservation. Her research activity developed mainly in Parma, with some research missions in Italy and abroad (Turkmenistan, China, Syria, Morocco, Albania, Luxembourg, and France). She is the author of more than 100 scientific papers and member of editorial committees of scientific papers and book series.

Erica Lenticchia is a Postdoctoral Fellow at the Politecnico di Torino (Italy), within the Earthquake Engineering and Dynamics Lab and member of the Responsible, Risk, Resilience Centre of the same university. She received a PhD in Architectural and Landscape Heritage from the Politecnico di Torino and was a Visiting Researcher at Columbia University, New York. She authored or co-authored more than 30 publications on seismic and structural analysis of existing RC and masonary structures, with special emphasis on structural health monitoring, seismic assessment, and preservation of both ancient and modern historical buildings.

Elena Michelini is an Assistant Professor of Structural Design at the University of Parma since 2016. She is an author of more than 60 papers on RC concrete and masonry structures (cracking, nonlinear analysis, tunnels, pre-cast RC elements, FRC, FRCM, AAC). She participated to several research projects funded by private companies or public administrations, mainly focused on the structural optimisation of new RC and FRC elements and on the vulnerability assessment of existing RC and masonry structures.

1 Introduction

Raw earth, in the form of sun-dried mud bricks, or adobe, as it is commonly known in various regions of the world, is one of the oldest and most widely used building materials. Thanks to its wide and cheap availability, its use is spread in all continents, giving rise to a large variety of building techniques and vernacular architectures, constituting a meaningful testimony of different civilisations, often resulting in precious cultural heritage assets (Avrami et al., 2008).

It is clear that adobe imposes precise limits of feasibility, but contrary to common beliefs, a large amount of technical and expressive goals has been reached with this construction material. The builders of the past have been able to significantly reduce the gap between the architectural idea and its related executive feasibility. Earthen architecture is widespread in the USA (Cancino et al., 2011; Tolles, 1996), Africa (Morris et al., 2004), Asia (Mecca and Dipasquale, 2009; Cacciavillani et al., 2017), and even in some parts of Europe (Correia et al., 2011). Tangible examples of the daring possibilities reached in the past are still present, despite this construction technique has

proven to be extremely vulnerable to earthquakes (Tolles et al., 2000; Almeida, 2012) and/or to scarce maintenance (Avrami et al., 2008).

The present paper describes the static structural analysis of a 2,000 year old dome built in adobe bricks. The dome was erected in the archaeological site of Old Nisa, in Turkmenistan, which was one of the first monumental centres of the Parthians. These nomadic people, coming from the Euro-Asiatic steppes, established in New Nisa their capital city, while Old Nisa was the fortified citadel of the sovereign Mithridates I the Great (171-138 BC). In Old Nisa, the building of the Round Hall, with its large circular area of 17 metres in diameter entirely made of adobe bricks (now exposed to the open sky), is generally interpreted nowadays as a building devoted to religious purposes (Invernizzi and Lippolis, 2008). However, its original conformation, and, in particular, the shape of its covering, remains a mystery to this day. The hypothesis of a large domed roof, already advanced by some scholars (Tolstov, 2002; Masturzo, 2008), is the most compelling. The significance of the building and the size of the dome are such that they would certainly have had considerable relevance at the time.

The shape of the dome can be a crucial clue for archaeologists and ethnographers to understand the Parthian architecture, which evolved from nomadic cultural traditions, thanks also to the confluence of the influences coming from Greek, Persian, and Central Asian architectures. Moreover, the dimensions of the dome seem a remarkable limit for a building material characterised by low mechanical performances. For this reason, in this work, the different hypotheses on the geometry of the dome made by archaeologists are analysed using the tools of structural analysis to validate or, possibly, to exclude the ones that are statically inadmissible.

Several works have been published on structural analysis of adobe constructions, especially in the seismic field (Aguilar et al., 2015; Cancino et al., 2011; Caporale et al., 2015; Lourenço and Pereira, 2018). In particular, finite element models typical of brick masonry have been adapted to the case of adobe masonry (Karanikoloudis and Lourenço, 2018; Miccoli et al., 2015; Parisi et al., 2019; Illampas et al., 2014; Tarque et al., 2012). Finite element models of adobe domes, however, are very few. Durá et al. (2012) analysed the structural behaviour of corbelled course domed houses. The authors observed that, despite the low mechanical properties of adobe masonry, the effect of gravitational loads is modest, and domes are capable of carrying a gravitational load higher than 2.5 times their weight. Rovero and Tonietti (2012) studied earthen corbelled domes in rural buildings in the Aleppo region (Syria). The authors observed that the good bond between adobe bricks and earthen mortar provided a monolithic behaviour of masonry that allowed to build thin domes that behave as ‘real domes’. Indeed, although the domes were built with corbelled layers of bricks arranged spirally, their small thickness was not compatible with the behaviour of a corbelled ‘false dome’ that is typical of tholoi.

The present paper is an extension of the research published in Blasi et al. (2008) motivated by the fact that studies reported in the literature in the last years have allowed to better define the behaviour of adobe masonry and its constitutive laws for finite element analysis. The paper is summarised as follows: Section 2 starts with the preliminary study on the possible geometries of the Old Nisa dome, Section 3 reports the mechanical characterisation of the adobe masonry employing in-situ testing; based on the findings reported in the previous sections, the structural analysis of the dome load-bearing capacity through FE macro-modelling is carried out in Section 4. Finally, Section 5 reports the discussion of the results and the conclusions of the work.

2 Possible geometries and proportions of the disappeared dome

The study of the possible geometries of the monumental complex of Old Nisa – the so-called Round Hall – starts from the geometric and technological analysis of the archaeological findings, reinterpreted in the light of historical documents and typological considerations. The obtained geometries are then analysed according to the outlook of building science and mechanics of materials, with the final aim to exclude statically unacceptable solutions.

The Round Hall building occupies a wide circular area with a diameter of 17 metres and is entirely made of adobe bricks. Nowadays, the building is uncovered; however, the analysis of similar buildings in the neighbouring regions makes scientists believe that the most plausible – and fascinating – hypothesis of roofing is that of a large adobe dome. Domes are indeed relatively common typological-constructive elements in the architecture of the Iranian area (Mecca and Dipasquale, 2009), also due to the lack of wood to produce large timber elements, and they can be found not only in historical buildings but also in vernacular structures, like icehouses and cisterns [Figure 1(a)], and in traditional houses [Figure 1(b)].

Figure 1 Examples of domes in the Iranian architecture, (a) typical Central-Asia icehouse (b) traditional house made of adobe bricks in Yazd, Iran (see online version for colours)

(a) (b)

Source: Roberto Coïsson

The remains of the Round Hall are shown in Figure 2(a). As can be seen, only the external walls of the building, forming the base of the dome, withstood the ravages of time. The building plan, reported in Figure 2(b), reveals that the geometry of the masonry basement is approximately square outside and round inside. Two masonry walls were subsequently added next to the north-west and south-west sides of the building. Since the dome must have resisted even without their presence (at least in a first period), these additional walls are not considered either in the preliminary study regarding the plan proportions, or in the structural analysis. The north side of the Round Hall leans against a masonry wall belonging to a pre-existing building, as demonstrated by the presence of plastering on its external surface. From the point of view of the proportions that govern the building, this wall represents an element of disturbance to the regularity in plan, but certainly it must have participated in the stability of the dome since its construction.

By looking at the plan, it can be noticed that the inner diameter of the circular hall approximately corresponds to half the diagonal of the outer square. Moreover, the minimum thickness of the wall section (s = 3.55 m) is almost one-fifth of the circle diameter and a tenth of the diagonal of the outer square [Figure 2(b)]. The latter proportion is less accurate due to the water washout that occurred during the centuries.

Figure 2 (a) Aerial view of Old Nisa and position of the Round Hall, (b) Study of its plan, to determine the possible proportions of the dome, based on the minimum masonry thickness *s* (c and d) General views of the Round Hall (see online version for colours)

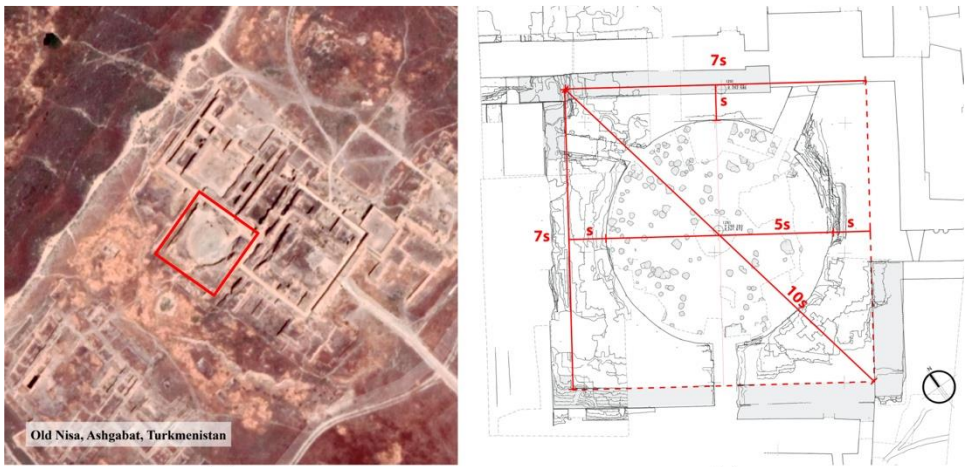

(a) (b)

(c) (d)

The geometrical survey of the remaining walls, which are approximately 3 m tall, highlights their uneven profile, proving that the original dome's curvature started from the ground (Figure 3). For this reason, the possible presence of a cylindrical tambour in the lower part of the construction, suggested by some Russian scholars (Tolstov, 2002), is not very likely.

Figure 3 (a) View of the east access of the building (b) Geometric survey of the wall sections, revealing that the curvature of the original dome started from the ground (see online version for colours)

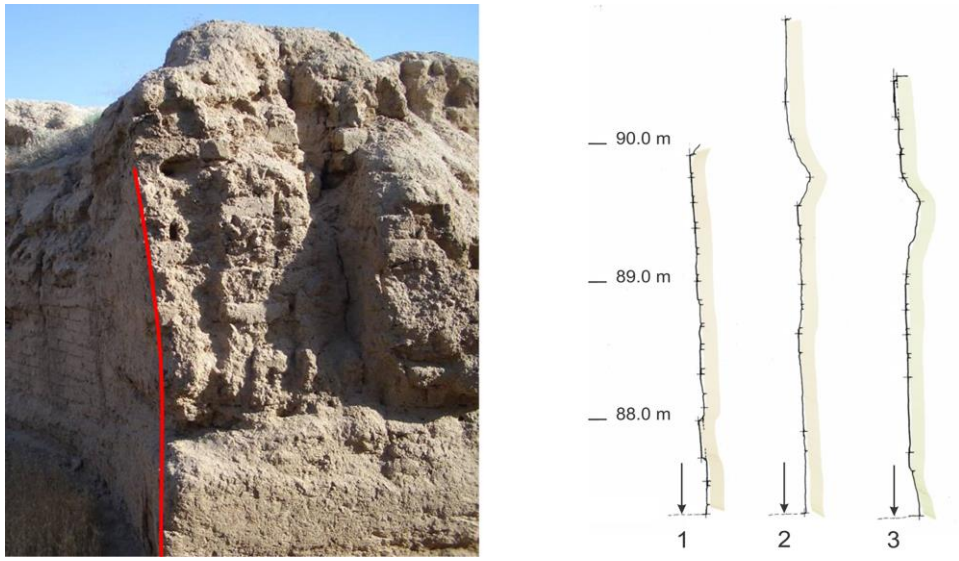

(a) (b)

2.1 Definition of the possible shapes and thickness of the Round Hall dome

The starting point for defining the most plausible geometries of the missing dome of the Round Hall is represented by the historical analysis of the Iranian architectural tradition, by identifying the construction typologies that are recurrent in the considered period. The oldest traces of large domes in the Central-Asian area go back to the third century BC, as testified by the ruins of the funerary building of Balandi II. Figure 4(a) shows its reconstruction, as performed by the archaeologist and ethnographer Tolstov (2002).

Figure 4 (a) Reconstruction of the site of Balandi II made by Tolstov (2002) (b) Example of vaulted system of the Sasanian period (Ctesiphon arch*)

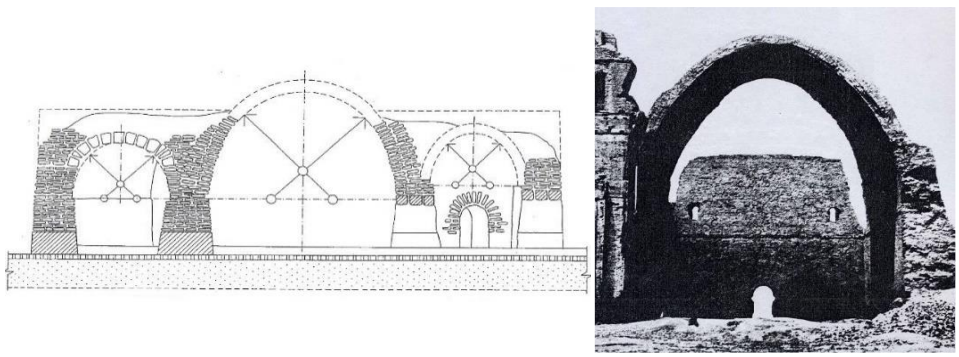

(a) (b)

Source: *Hernández-Montes et al. (2017)

Another typical Iranian architectural element is the vaulted system, realised with inclined brick courses resting on three massive walls, which does not require the use of timber centring. Even if this technique dates back to the Parthian era, one of the finest examples of its application can be found in the Sasanian period (3rd–6th century AD), in the Ctesiphon arch [Figure 4(b)], covering a span of 23 m with a parabolic section. Dating from the same period is the Bishapur Palace, whose throne room was probably covered by an impressive 25 m high dome, according to the reconstruction of Ghirshman, reported in Figure 5(a) (Ghirshman et al., 1962). Until that period, all domes rested on an internally circular basis, while the great revolution of Sasanian architecture is the introduction of the pendentives, which allow the realisation of a circular dome on a square basement. One of the first and rarest surviving examples of this technique, even if partially in ruins, is the Ardashir Palace in Firuzabad [Figure 5(b)], dating back to the 3rd century AD. From that period onwards, circular domes on square bases are commonly used not only for monumental architectures, but also for the covering of traditional residential buildings in small cities and villages, like the city of Bam in the southeast of Iran (Maheri, 2005; Hejazi, 1997). Also corbelled dome buildings with different geometries become quite widespread, as discussed in Dipasquale et al. (2009).

It should be noted that the definition of the dome geometry is not merely limited to identify its shape, but also involves the choice of its thickness, which is generally variable from the base to the top. A larger thickness gives indeed greater strength to the structure, but also higher dead loads. Thus, different thickness distributions may give rise to a different structural behaviour, while retaining the same shape of the intrados surface of the dome.

Figure 5 (a) Reconstruction of the throne room of the Bishapur Palace made by Ghirshman et al. (1962) (b) Sasanian Palace of Ardashir, in Firuzabad* (see online version for colours)

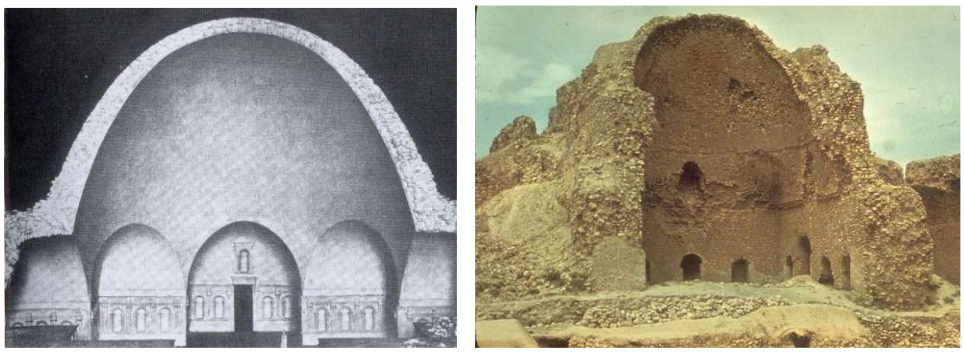

(a) (b)

Source: *Pope (1930)

Rovero and Tonietti (2012) describe a building in which the square base is made of large adobe bricks. Instead, the dome is built with thinner adobe bricks (5–6 cm) characterised by a more regular geometry. These bricks are arranged overhanging on inclined bedjoints, thus reducing the shear action parallel to the joint plane and improving the

shear performance of the masonry, thanks to the higher normal stress component. Moreover, as aforesaid, the good bond observed between adobe bricks and earthen mortar provides a monolithic behaviour of the dome masonry.

Figure 6 (a) Brick layout at the base of the Round Hall (the white lines indicate the expected base of the dome) (b) Brickworks at the impost of the vaulted covering placed over the north-west access of the Round Hall, with bricks arranged along inclined courses (see online version for colours)

(a) (b)

In the present work, it is decided to decouple the two problems of shape and thickness definition, by setting some general criteria to be applied preliminarily to all the case studies examined in numerical analyses, independently from the chosen shape. First, it is always assumed an increasing thickness from the top to the bottom of the dome, since this stabilising construction criterion was probably already known during the Parthian period (it was applied a few centuries later in the cited cases of the Ardashir Palace and of the Ctesiphon Arch). Moreover, the minimum thickness in the upper part of the dome is assumed equal to 0.44 m, namely the side of a brick. This assumption derives from the observations made during the in situ surveys on the Round Hall and on the remains of a vaulted covering found nearby, which suggest that the Parthians were acknowledged with the use of inclined mortar beds. Parthians probably applied it also in the construction of the dome, thus entailing the presence of vertical bricks in the crown and justifying the assumption of the minimum thickness of the dome equal to the brick side. The survey of the brick arrangement in the bottom part of the dome [Figures 6(a)–6(b)] highlights that only three rows of bricks – corresponding to a total thickness of 1.32 m – follow the curvature of the hall in plan [as evidenced with white lines in Figure 6(a)], thus being part of the true and proper structure of the dome. Consequently, 1.32 m is the thickness assumed at the dome impost in all the considered cases. The overall thickness of the base is assumed equal to 3.55 m according to the proportion studies, while its height is set equal to 6 m.

Figure 7 Dome profiles considered in numerical analyses, (a–c) preliminary proposals made by Masturzo (2008) based on situ surveys (d) profile reported in 'Masterpiecees of Iranian architecture' by Eshragh and Society of Iranian Architects (1970) (e) simple semi-spherical profile without drum (f) scaled reproduction of the section of Sasanian Palace of Taq-I Kisra in Ctesiphon (g) reconstruction of the throne room of Bishapur Palace, by Ghirshman et al. (1962) (h) profile proposed by Tolstov (2002) (i) semi-spherical profile with drum (l–o) variants of the reconstruction made by Masturzo (2008) (see online version for colours)

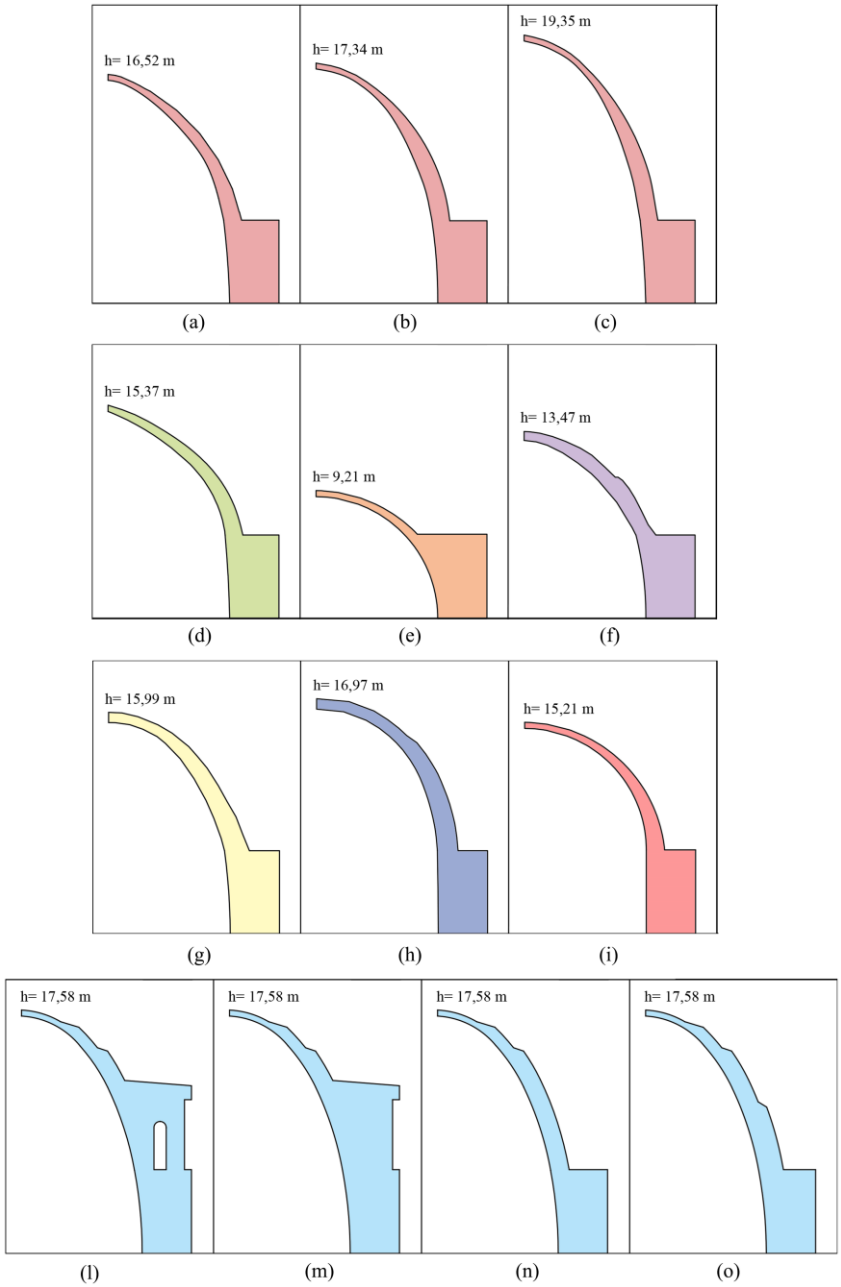

Against this background, the dome profiles considered in the present work are those reported in Figure 7. As can be seen, three possible shapes are studied: elliptical, semi-circular, and parabolic, by keeping the dome internal radius equal to 8.77 m and varying its height from 9.21 m to 19.35 m. In more detail, profiles in Figures 7(a), 7(b), and 7(c) correspond to some preliminary proposals made for the Round Hall by Masturzo (2008) on the basis of his in situ surveys. The solution in Figure 7(d) is taken from Eshragh and Society of Iranian Architects (1970), although it should be observed that the cusp at the crown is an architectural element that would have developed only later on in the Persian scene. Case study in Figure 7(e) represents a simple semi-spherical profile without drum, Figure 7(f) is a scale reproduction of the vaulted section of the Sasanian Palace of Taq-i-Kisra in Ctesiphon [Figure 4(b), Hernández-Montes et al., 2017], Figure 7(g) follows the reconstruction of the throne room of the Bishapur Palace made by Ghirshman et al. (1962), Figure 5(a). Moreover, the elliptical shape adopted in Figure 7(h) derives from the proposal of the Russian scholar Tolstov (2002), on the basis of the archaeological findings of Balandi II, Figure 4(a), Figure 7(i) is a semi-spherical profile with drum, according to the solution proposed by Russian scholars for the Round Hall, while Figures 7(l), 7(m), 7(n) and 7(o) are variants of the reconstruction made by Masturzo (2008), with or without a gallery and with a different arrangement of the steps. For a more detailed analysis of the proposed profiles, the reader can refer to Masturzo (2008).

3 Mechanical characterisation of adobe masonry through in-situ testing

Once the possible geometries for the Round Hall dome are defined, the subsequent step to prepare the numerical model consists in the calibration of suitable constitutive laws to describe masonry behaviour in tension and compression. In situ surveys highlighted that the Round Hall walls are made of sun-dried adobe bricks, with dimensions equal to 440 mm × 440 mm × 120 mm. Those bricks are formed by a mixture of clay, silt, and gravel originally additioned with dung and straw (now completely dissolved), characterised by a specific weight approximately equal to 18 kN/m^3. Adobe bricks are connected through mortar bedjoints and headjoints, with a mean thickness of 40–50 mm. Mortar has a similar composition to that of bricks.

Despite the availability of several experimental data on adobe masonry in the technical literature (Chasagnoux, 1996; Caporale et al., 2015; Parisi et al., 2015), it was deemed appropriate to characterise some material samples directly taken from the archaeological site, given its peculiar origin and history. The characteristics of adobe masonry can indeed be subjected to significant variations, related to its components and their proportion in the admixture, but also to the age and the weathering conditions. The results of the experimental testing campaign on the material of the Round Hall, reported in Adorni et al. (2013), are briefly summarised here for convenience. In particular, the mineralogical and petrographic analyses showed that the bricks of the Round Hall were made with local soil. The material consisted of clay and silt, with abundant fragments of rock. In addition, there were animal dung and straw, now degraded (Adorni et al., 2013). The determination of the mechanical properties through destructive tests on large masonry elements is not feasible in the case of archaeological heritage, already very limited in its remains; for this reason, it was decided to characterise the behaviour of the masonry components. Moreover, due to the similarities between mortar and bricks in

terms of composition, it seemed reasonable to focus the attention exclusively on bricks, which usually govern adobe masonry behaviour.

Given the difficulties of transferring material samples to a material testing laboratory, it was preferred to organise the experimental campaign directly onsite by using small portions of bricks extracted by the archaeologists. Apart from density measures, the experimental program consisted in compression tests on seven prismatic specimens with dimensions approximately equal to 60 mm × 60 mm × 99 mm, six three-point bending flexural tests on small beams with average dimensions of 81.6 mm × 61 mm × 110 mm, and seven splitting tensile tests on cylindrical specimens about 81 mm in diameter and 78.7 mm in height. The reported dimensions should be intended as average values for each type of testing, because the specimens showed moderate variability due to the irregular structure of the material and the frequent presence of rock inclusions.

All the tests were performed using a portable testing machine designed on purpose (Figure 8), made of two aluminium bases connected with three adjustable steel columns, and working as a press. The force was applied by turning a fine-pitch screw with a wrench. The screw acted on a 10 kN portable load cell, connected to the load platen of the testing machine (Figure 8). Displacements were not directly measured on specimens, but they were obtained indirectly from those of the load platen. These latter displacements were computed by measuring the rotations of the screw with a 360° protractor marked in degrees. Calibration in the laboratory showed that this instrument can measure forces with an accuracy of 0.1 N and load-platen displacements with an accuracy of 0.01 mm. A detailed description of the adopted instrumentation and the performed tests can be found in Adorni et al. (2013).

Figure 8 On site mechanical tests on adobe bricks of the Round Hall, (a) compression tests (b) three-point-bending tests (c) Brazilian tests (see online version for colours)

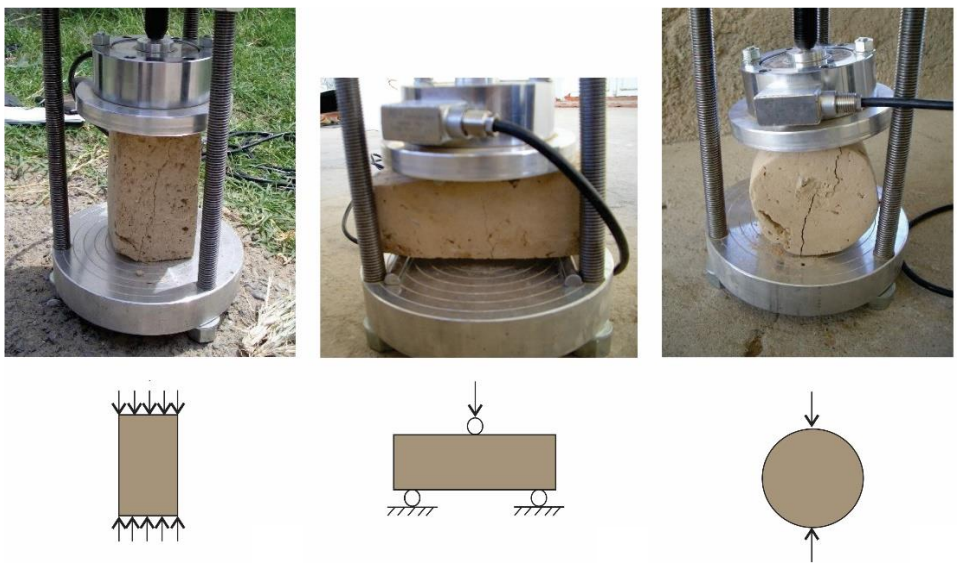

(a) (b) (c)

Source: Adapted from Adorni et al. (2013)

Table 1 Mechanical properties of specimens obtained from in-situ tests on ancient adobe bricks

Ref.	ρ *(kg/m³)*	λ	f_c *(MPa)*	E_g *(MPa)*	$f_{t,fl}$ *(MPa)*	$f_{t,spl}$ *(MPa)*	f_t *(MPa)*	G_F *(N/mm)*
Adorni et al. (2013)	1,750	1.8	1.04	215.6	0.29	0.20		
Aguilar et al. (2015)	1,750		1.16	147.0	0.58	0.25		0.024
Almeida (2012)		2.0	1.18				0.081	0.0147
Baglioni et al. (2010)			2.15		0.27			
Eslami et al. (2012)		0.25	6.00					
Figueiredo et al. (2012)	1,600		0.46				0.15	
Fratini et al. (2011)		1.0	0.50	59.1				
Martins and Varum (2006)		2.0	1.01	176.3		0.13		
Rivera Torres (2012)	1,770		3.04		0.41			
Silveira et al. (2012)		2.0	1.13	185.9		0.19		
Silveira et al. (2013)	1,433	1.8	0.58		0.56	0.16		
Silveira et al. (2013)	1,433	1.0	0.54					
Silva et al. (2020)	1,764	0.67	0.85		0.44			

The main results of the tests are summarised in Table 1, where they are also compared with experimental data on ancient adobe bricks available in the literature. The table includes only tests on bricks taken from archaeological sites or historical buildings. In particular, ρ represents the specific density, λ is the ratio between height and diameter/base of the samples in compression, f_c is the compressive strength, E_g is the Young's modulus, $f_{t,fl}$ is the flexural tensile strength, $f_{t,spl}$ is the splitting tensile strength, f_t is the direct tensile strength, and G_F is the fracture energy in tension. It can be noticed that, for the same density, the mechanical characteristics are similar, as already observed by Morel et al. (2007).

The calibration of the constitutive laws describing the mechanical behaviour of the adobe blocks used in the Round Hall can also be found in Adorni et al. (2013). The adopted relations are here briefly recalled for reading convenience. To describe the behaviour in uniaxial compression, the stress-strain curve proposed by Popovics (1973) is used:

$$\frac{\sigma}{\sigma_{\max}} = \frac{n\left(\frac{\varepsilon}{\varepsilon_u}\right)}{n-1+\left(\frac{\varepsilon}{\varepsilon_u}\right)^n} \tag{1}$$

being $\sigma_{\max}$ = 1.04 MPa the peak stress (CV = 0.14), ε_u = 0.67% the corresponding strain, and assuming a coefficient n = 4.1, based on the available data deriving from in situ tests. The behaviour in tension is assumed linear elastic up to cracking, with Young modulus E_g = 215.6 MPa (CV = 0.19). Three-point bending tests provided a flexural strength $f_{t,fl}$ = 0.29 MPa (CV = 0.32), whereas Brazilian tensile strength was $f_{t,spl}$ = 0.2 MPa (CV = 0.32).

Table 2 Mechanical properties of adobe masonry, bricks and mortar

Ref.	*Bricks*			*Mortar*			*Masonry*		
	ρ (kg/m^3)	f_c *(MPa)*	E_g *(MPa)*	ρ (kg/m^3)	f_c *(MPa)*	E_g *(MPa)*	ρ (kg/m^3)	f_c *(MPa)*	E_g *(MPa)*
Aguilar et al. (2015)	1,750	1.16	147	1,990	2.33	293	1,735	0.36	115
Abdulla et al. (2020)	1,855	1.59						1.24	127
Almeida (2012)		1.18	1,138		2.67			1.47	2,059
Arrojo-Matus et al. (2013)	-	1.10	-	-	0.93	289	-	0.97	312
Miccoli et al. (2015)	1,870	5.21	2,197		3.32	1,067		3.28	803
Pereira (2008)	-	0.99–2.15	161–448	-	1.42	-	-	0.86–1.33	173–200
Piattoni et al. (2011)		2.55	131					1	33
Silva et al. (2020)		0.85						0.45	
Torrealva et al. (2018)	-	0.59–1.35	-	-	-	-	-	0.39–0.76	-
Varum et al. (2012)	-	0.45	-	-	0.47	-	-	0.33	-
Varum et al. (2015)	-	0.7–2.15	87–448	-	1.19	128–251	-	0.59	-
Wu et al. (2012)		1.66			1.58			0.94	

The values obtained for the bricks are useful, however, they are not coincident with masonry properties. Table 2 shows a comparison between the mechanical parameters of masonry and of its components measured in some experimental campaigns from the literature. As can be observed, in the case of bricks with density and resistance close to those of the bricks under examination, Aguilar et al. (2015) have measured a compressive strength of the masonry that is about one third of the compressive strength of the bricks. However, the analysis of the scant experimental data in Table 2 shows a mean factor of 0.6 between the compressive strength of masonry and that of bricks. The coefficient 0.6 is roughly valid for the Young modulus E_g. Based on these observations, in the FE analyses described in the following section we have decided to adopt different mechanical properties for masonry and bricks. This is the major departure from the work of Blasi et al. (2008), in which the mechanical parameters of the masonry were taken equal to those of the bricks, because of the lack of experimental data at the time.

4 Structural analysis of the dome through FE macro-modelling

The evaluation of the load bearing capacity of the Round Hall dome requires the construction of 13 different FE models, corresponding to all the geometries hypothesised in Figure 7. To this aim, the commercial software ABAQUS (Simulia, 2018) is adopted. In order to avoid complex and time-consuming three-dimensional analyses, it is decided to consider the problem as axisymmetric. This assumption seems reasonable due to the massive structure of the dome base, which allows approximating its square plan with a circular one, by considering negligible the contribution offered by the corners. The axisymmetric condition is also consistent with the assumptions made on the applied loads. In this study, only the effect of vertical loads on the load bearing capacity is indeed analysed, by implicitly assuming that the shape of the dome was governed by static considerations. Thus, only the self-weight is applied to the structure. If the dome, in virtue of its shape, is able to sustain the self-weight without collapsing, it is possible to gradually increase the applied load during the analysis until failure. In this way, the structural efficiency of the different dome shapes can be compared through the definition of a load multiplier Fs, which is set equal to the ratio between collapse load and self-weight. The effects of seismic and thermal actions, although important given the area where the dome stood, are not taken into account because they are out of the scope of this paper.

4.1 Modelling assumptions

As depicted in Figure 9(a), a mesh with quadrangular axisymmetric solid finite elements (named CAX 4R) is adopted. Following the crack band approach, mesh sensitivity is reduced by using elements of the same size (approximately 170 mm).

The model is assumed to be fixed at the foundation level by blocking vertical and horizontal displacements between the structure and the ground. As proved by preliminary numerical studies, the heavy vertical loads acting on the structure prevent indeed the slip between the structure itself and the ground below, even when their interaction is explicitly modelled through a Coulomb type contact. Geometric nonlinearity is included in the model, although the displacements of the structure are modest. Masonry is modelled as an isotropic and homogeneous material by following a macro-modelling

approach. The 'concrete damaged plasticity' (CDP) model, available in ABAQUS code, is adopted to describe the nonlinear mechanical behaviour of masonry. Despite its name, this model is not only applicable to concrete structures, but provides a general capability for modelling also other quasi-brittle materials, like masonry (D'Altri et al., 2017; Zanazzi et al., 2019).

Figure 9 Finite element analysis of dome profile 'a' subjected to self-weight, (a) mesh (b) maximum in-plane principal stress (c) minimum in-plane principal stress (d) out-of-plane principal stress (stresses are in N/mm^2) (see online version for colours)

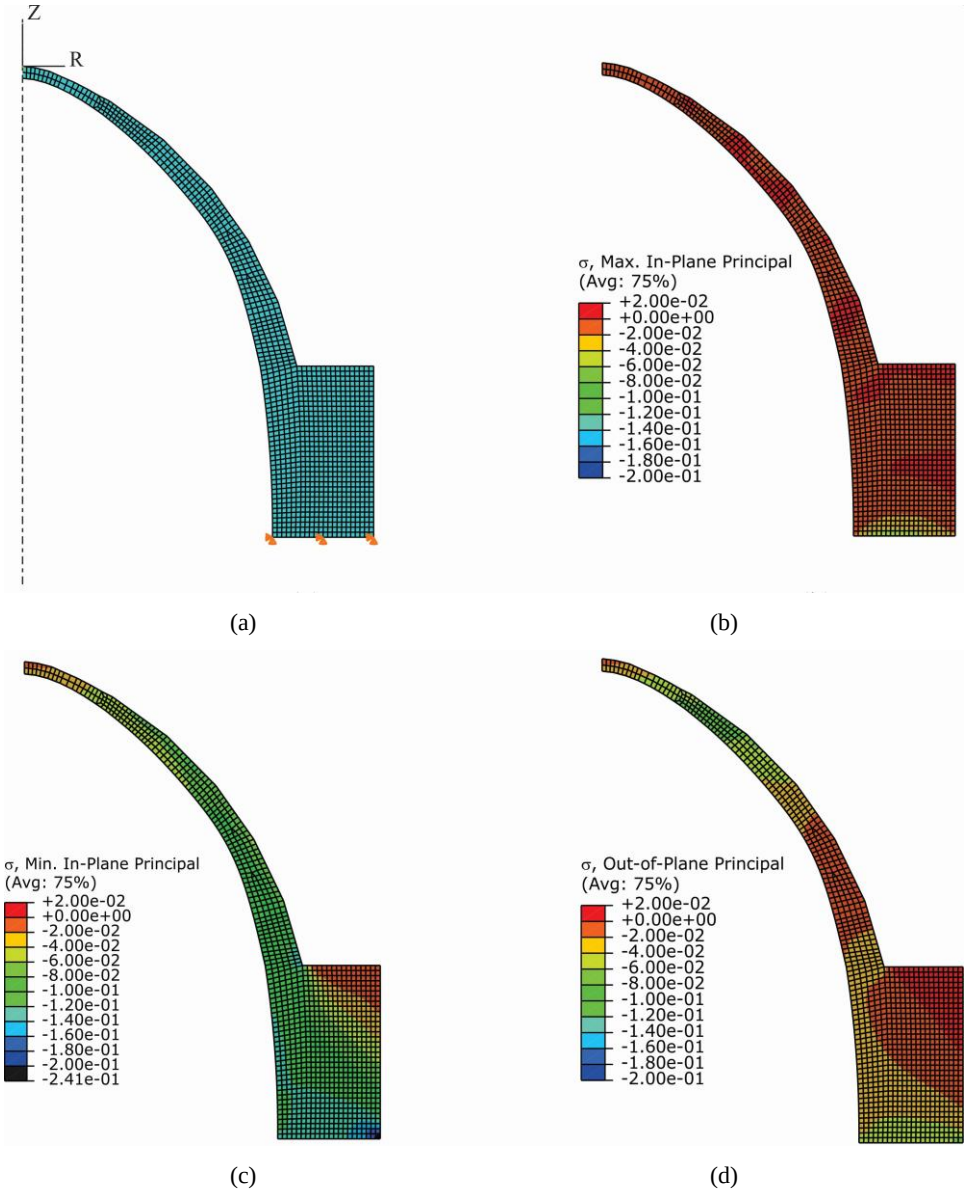

(a) (b)

(c) (d)

CDP is a continuum, plasticity-based damage model, assuming two main failure mechanisms, i.e., tensile cracking and compressive crushing, for the material. To this aim, it is necessary to define the uniaxial tension and compression stress-strain laws. In the present work, for the compressive behaviour the constitutive law measured on bricks is adopted [equation (1)], by rescaling it with a coefficient equal to 0.6. As already mentioned, this coefficient derives from the analysis of the experimental data reported in Table 2.

For the tensile behaviour, the law proposed by Tarque et al. (2012) is adopted, by assuming that the mortar-brick adhesion is not very good, and therefore the tensile strength of bricks does not represent the behaviour of masonry. The resulting laws are represented in Figure 10 in terms of stresses vs. plastic strains. The same figure shows the damage – plastic strain laws.

Figure 10 Stress-strain curves adopted in the FE analyses for modelling masonry behaviour in (a) compression and (b) tension (see online version for colours)

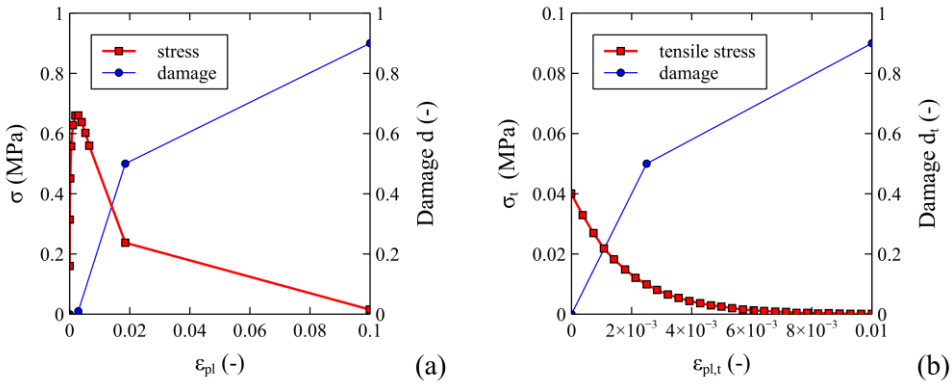

Concerning the modelling of the material behaviour under a biaxial or triaxial state of stress, the definition of the yielding surface in ABAQUS requires the calibration of four parameters. For three of them, standard values suggested in the literature are assumed: the ratio between biaxial and uniaxial compressive strength σ_{b0}/σ_{c0} is posed equal to 1.16; the ratio between second stress invariant on the tension meridian and second stress invariant on compression meridian K_c is set equal to 0.667 (K_c being important in triaxial compression only); and the eccentricity of the plastic potential surface ε is set to the default value of 0.1. These values, which are the standard ones suggested for concrete (Jankowiak and Lodygowski, 2005), are usually satisfactorily applied to the analysis of masonry elements (see, i.e., Resta et al., 2013; Dauda et al., 2018; Bhosale and Desai, 2019).

Regarding the last parameter, the dilation angle ψ, a general agreement has not been reached within the scientific community about the most suitable value for describing masonry behaviour, and values ranging between 1° and 30° can be found. Resta et al. (2013) and Wosatko et al. (2019) observed that the dilation angle significantly affects the results of FE models and that for values ranging from 30° to 37°, the material exhibits a ductile behaviour, while for values close to zero, the behaviour is brittle. In this work, a value of ψ = 10° is assumed, according to D'Altri et al. (2017) for solid clay masonry and Illampas et al. (2014b) for adobe masonry. Finally, the viscosity parameter υ, which

affects the numerical stability of the constitutive law, is set equal to 0.0002 (see, e.g., D'Altri et al., 2017).

4.2 Load bearing capacity of domes under the self-weight

The first step in the topological study of the dome shape consists in the analysis of its load-bearing capacity under the self-weight: all the geometries that cannot sustain this load are obviously unacceptable from a static point of view and should be discarded. To this aim, the in-plane and out-of-plane principal stresses in each dome typology are examined (in the following, tension is considered as positive). For the sake of brevity, Figure 9 only shows the contours relative to the case of the dome according to Figure 7(a).

Figure 11 Finite element analysis of dome profile at collapse, (a) maximum in-plane principal strains (b) minimum in-plane principal strains (c) out-of-plane principal strains and (d) plastic strain magnitude PEMAG (see online version for colours)

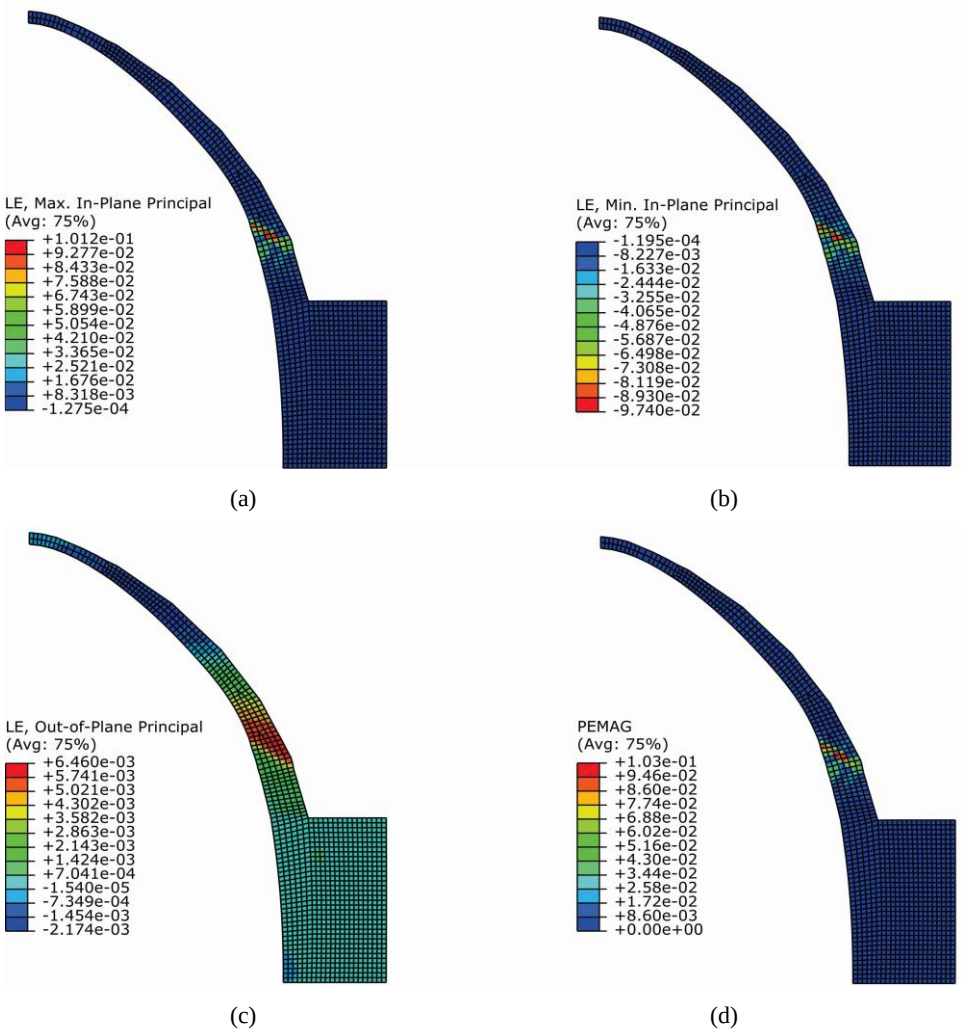

As can be observed in Figure 9, the maximum and minimum principal stress values do not exceed the corresponding masonry strengths in tension and compression, which are respectively equal to $\sigma_{t,\max}$ = 0.04 MPa and $\sigma_{\max}$ = 0.66 MPa [Figures 9(b) and 9(c)].

Near the impost of the dome, where the profile tapers, a limited stress concentration takes place, but not such as to cause concern. Figure 9(d) highlights that out-of-plane stresses are relatively low, too. As expected, the lower part of the dome is subjected to tension, while the upper one is compressed. Based on these results, it can be argued that the considered dome profile is acceptable from a static point of view since it does not show cracking nor compression crushing under its self-weight.

Similar results are also found for all the other examined dome profiles of Figure 7. Maximum in-plane principal stresses span values comprised between 0.01–0.03 MPa, whereas minimum in-plane principal stresses range between –0.13 and –0.25 MPa.

Finally, out-of-plane tensile stresses, which tend to divide the dome into separate segments, can be observed for the geometries reported in Figures 7(a), 7(d), 7(g), 7(h), 7(i), 7(m), and 7(o). Nevertheless, the check on stresses reveals that cracking onset does not occur yet at this loading level.

4.3 FE analyses up to failure and structural efficiency of the different dome profiles

The topological optimisation of the dome profile requires identifying the best shape and thickness – among those that are historically plausible – which allow sustaining the applied loads while minimising the self-weight. To this aim, FE analyses on the 13 possible domes reported in Figure 7 are repeated, by increasing the applied loads up to failure. Based on the obtained results, the efficiency of a given profile can be evaluated by analysing two different parameters, which are the maximum vertical load multiplier F_s, and the crack pattern (and consequently the damage distribution) within the dome.

Table 3 Evaluation of the efficiency of the considered dome profiles in terms of maximum vertical load multiplier F_s

Dome profile	*F_s (–)*	*Collapse mechanism*
a	6.78	I
b	5.28	I + II
c	4.50	II
d	6.34	II
e	8.46	I + II
f	6.04	I
g	5.47	II
h	5.11	I + II
i	5.11	II
l	4.05	III
m	3.02	II
n	4.50	II
o	5.39	I + II

Note: For each considered case, the observed failure mechanism is also specified.

Figure 12 Different collapse mechanisms observed in FE analyses, (a) collapse mechanism I, profile f (b) collapse mechanism II, profile d (c) collapse mechanism I + II, profile b (d) collapse mechanism III, profile l (see online version for colours)

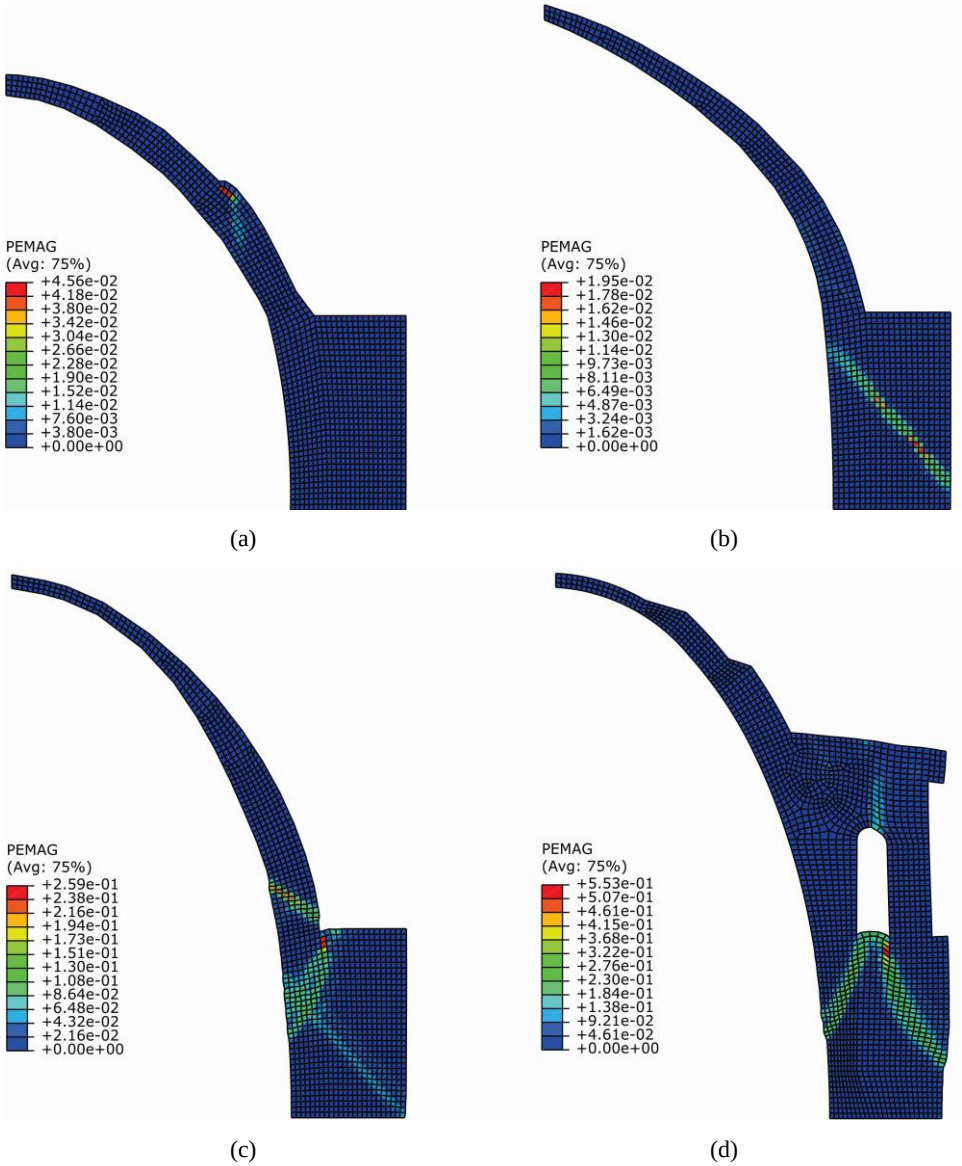

The load multiplier F_s is calculated as the ratio between the maximum sustained vertical load and the self-weight of the structure; consequently, higher values of F_s correspond to more efficient profiles. Given a fixed bearing capacity, a structure with a lower self-weight can be indeed considered more efficient, since it allows economic savings on materials and labour, and reduces the time required for the construction. The values of load multiplier F_s obtained from numerical analyses are reported in Table 3. The results highlight that the more efficient profiles are those corresponding to the preliminary

proposals made by Masturzo (2008) on the basis of his in situ surveys [domes in Figures 7(a), 7(b) and 7(c)], while domes Figures 7(l), 7(m), and 7(n) are penalised by the presence of the massive drum, which collapses under its own vertical load rather than for the action of the dome.

Finally, the attention is focused on the possible failure modes obtained from numerical analyses. Generally speaking, crack pattern and damage distribution can be another factor to be considered when judging structural efficiency: on one side, a severe and concentrated crack pattern could have suggested 'experimentally' to the ancient builders to change the adopted technical solutions; on the other side, the more widespread is the damage, the better is the structural behaviour, thanks to the larger exploitation in the inelastic field. This latter aspect can provide a rough indication about the potential for damage also in case of seismic actions, which are, however, out of the scope of this work.

For the analysed domes, three main collapse mechanisms can be identified, according to Figure 12, where the cracked areas are shown by the plot of the plastic strain magnitude PEMAG. Collapse mechanism I [Figure 12(a)], which is typical of profiles (a) and (f), is characterised by damage concentration in the dome, usually close to geometric discontinuities (thickness variation or impost).

Mechanism II [Figure 12(b)] can be found in domes (c), (d), (g), (i), (m), and (n): in this case, cracking is concentrated in the base. In other cases [like domes (b), (e), (h), (o)], a single failure mechanism is hardly distinguishable, and the collapse is attributable to a mix of them, with a larger extension of the damaged area [Figure 12(c)]. Finally, profile (l) displays a specific damage mechanism around the openings [Figure 12(d)].

Numerical results show a low stress state and the absence of cracking under self-weight for all the 13 profiles. Rovero and Tonietti (2012) achieved the similar results for their domes. In addition, all 13 profiles are able to carry their own weight with a large safety margin, similarly to what was observed by Durá et al. (2012).

5 Conclusions

This work analyses the possible geometries of the disappeared adobe dome covering the Round Hall building in the archaeological site of Old Nisa, in present-day Turkmenistan. Thirteen possible profiles are first identified starting from a preliminary study of the geometry, techniques, and proportions of the examined building, supplemented with the historical analysis of the architectural tradition of the area and the identification of the construction typologies that were more recurrent in the considered period.

The structural efficiency of these possible dome profiles is subsequently investigated through nonlinear finite element analyses. In order to calibrate the material constitutive laws adopted in FE analyses, an experimental program was carried out onsite, to characterise archaeological adobe bricks behaviour in tension and compression. Thanks to the similar composition of the bricks and of the mortar between them, the mechanical properties of the bricks are scaled down to define the behaviour of masonry, which is modelled as a single isotropic and homogeneous material. Obviously, the tested specimens were extracted from an archaeological material that withstood the ravages of time, and consequently, the corresponding mechanical properties are referred to its present-day condition. It seems reasonable that the behaviour of the original material has been different, and most likely better, due to the presence of straw fibres originally included in the admixture. These straw fibres have decomposed during the centuries,

leaving small holes and voids within the bricks, and certainly reduced their mechanical performances.

Based on the obtained numerical results, the following conclusion can be drawn:

- All the considered geometries are acceptable from a static point of view since the domes can effortlessly stand their own self-weight.
- All the considered domes are able to sustain a vertical load at least equal to 3 times their self-weight. Based on the values of the maximum vertical load multiplier obtained from the analyses, the most efficient profiles seem to be the profiles in Figures 7(a), 7(d), 7(e), and 7(f).
- Two main collapse mechanisms can be identified, respectively characterised by damage concentration in the dome (mode I) or at the base (mode II). However, most of the examined geometries show a mixed failure mode, with widespread cracking (modes I + II). A third collapse mechanism regards profile l, with crack concentration near the openings.

The analyses do not allow to exclude some geometries among the 13 analysed, because all of them are able to safely carry their own weight. Despite the low mechanical properties of adobe masonry, the choice of the dome geometry does not seem to be a critical element, and this would support even more the hypothesis of a dome cover for the Round Hall.

Acknowledgements

This research benefits from the high performance computing (HPC) facility of the University of Parma, Italy.

References

Abdulla, K.F., Cunningham, L.S. and Gillie, M. (2020) 'Experimental study on the mechanical properties of straw fiber–reinforced adobe masonry', *Journal of Materials in Civil Engineering*, Vol. 32, No. 11, p.04020322.

Adorni, E., Coïsson, E. and Ferretti, D. (2013) 'In situ characterization of archaeological adobe bricks', *Construction and Building Materials*, March, Vol. 40, pp.1–9.

Aguilar, R., Marques, R., Sovero, K., Martel, C., Trujillano, F. and Boroschek, R. (2015) 'Investigations on the structural behaviour of archaeological heritage in Peru: from survey to seismic assessment', *Engineering Structures*, July, Vol. 95, pp.94–111.

Almeida, J.A.P.P. (2012) *Mechanical Characterization of Traditional Adobe Masonry Elements*, Master thesis in Structural Analysis of Monuments and Historical Constructions, University of Minho, Portugal.

Arrojo-Matus, R., Sánchez Tizapa, S. and Catalán Quiroz, P. (2013) 'Experimental determination of the mechanical properties of adobe masonry from the South of Mexico', *Ingeniería*, in Spanish, Vol. 17, No. 3, pp.167–177.

Avrami, E., Guillaud, H. and Hardy, M. (2008) *Terra Literature Review: An Overview of Research in Earthen Architecture Conservation*, Getty Conservation Institute, Los Angeles CA.

Baglioni, E., Fratini, F. and Rovero, L. (2010) 'The materials utilised in the earthen buildings sited in the Drâa Valley (Morocco): mineralogical and mechanical characteristics', in *Proceedings 6° Seminario Arquitectura Terraem Portugal 9°Seminario Ibero Americano Arquitectura e Construção com Terra*.

Bhosale, S.D. and Desai, A.K. (2019) 'Simulation of masonry wall using concrete damage plasticity model', *International Journal of Innovative Technology and Exploring Engineering*, Vol. 8, No. 953, pp.1241–1244.

Blasi, C., Coïsson, E. and Ferretti, D. (2008) 'Nisa Partica: Ricerche nel complesso monumentale arsacide 1990-2006, N. 9 Monografie di Mesopotamia', in Invernizzi, A. and Lippolis, C. (Eds.): *Nisa Partica – Ricerche nel complesso Monumentale arsacide*, Le Lettere, Firenze.

Cacciavillani, C., Rinaldi, S. and Severini, M. (2017) 'Vernacular construction techniques and earth employ in Arg-e-Bam (Iran)', in *Vernacular Earthen Architecture: Conservation Sustainability*, pp.59–64, Sos Tierra 2017, Valencia, Spain, 1416 September.

Cancino, C., Farneth, S., Garnier, P., Vargas, J. and Webster, F. (2011) *Damage Assessment of Historic Earthen Buildings after the August 15, 2007 Pisco, Peru Earthquake*, Getty Conservation Institute, Los Angeles, CA.

Caporale, A., Parisi, F., Asprone, D., Luciano, R. and Prota, A. (2015) 'Comparative micromechanical assessment of adobe and clay brick masonry assemblages based on experimental data sets', *Composite Structures*, February, Vol. 120, pp.208–220.

Chasagnoux, A. (1996) *L'architecture voûtée iranienne – modélisation et simulation par éléments finis*.

Correia, M., Dipasquale, L. and Mecca, S. (Eds.) (2011) *Terra Europae: Earthen Architecture in the European Union*, ETS, Pisa, Italy.

D'Altri, A.M., Castellazzi, G., de Miranda, S. and Tralli, A. (2017) 'Seismic-induced damage in historical masonry vaults: a case-study in the 2012 Emilia earthquake-stricken area', *Journal of Building Engineering*, September, Vol. 13, pp.224–243.

Dauda, J.A., Iuorio, O. and Lourenço, P.B. (2018) 'Characterization of brick masonry: study towards retrofitting URM walls with timber-panels', in Milani, G. (Ed.): *10th International Masonry Conference (10thIMC)*, IMC, Milan, Italy.

Dipasquale, L., Mileto, C. and Vegas, F. (2009) 'Earthen domes et habitats: villages of northern Syria', in *Earthen Domes Habitats*, pp.267–285, Edizioni ETS, Pisa.

Durá, A., Boquera, A.M. and Pulido, L. (2012) 'Analysis and characterization of earthen architecture as a structural material: the corbelled course domes in Syria', in Mileto, C., Vegas, F. and Cristini, V. (Eds.): *Rammed Earth Conservation Proceedings First International Conference Rammed Earth Conservation*, CRC Press, pp.461–466.

Eshragh, A.H. and Society of Iranian Architects (1970) *Masterpieces of Iranian Architecture*, Ministry of Development and Housing with the cooperation of the Society of Iranian Architects.

Eslami, A., Ronagh, H.R., Mahini, S.S. and Morshed, R. (2012) 'Experimental investigation and nonlinear FE analysis of historical masonry buildings – a case study', *Construction and Building Materials*, October, Vol. 35, pp.251–260.

Figueiredo, A., Varum, H., Costa, A., Silveira, D. and Oliveira, C. (2012) 'Seismic retrofitting solution of an adobe masonry wall', *Materials and Structures*, Vol. 46, Nos. 1–2, pp.203–219.

Fratini, F., Pecchioni, E., Rovero, L. and Tonietti, U. (2011) 'The earth in the architecture of the historical centre of Lamezia Terme (Italy): characterization for restoration', *Applied Clay Science*, Vol. 53, No. 3, pp.509–516.

Ghirshman, R., Gilbert, S. and Emmons, J. (1962) *Persian Art, The Parthian and Sassanian Dynasties*, 249BC-AD651, Golden Press, New York.

Hejazi, M. (1997) *Historical Buildings of Iran: Their Architecture and Structure*, Computational Mechanics Publication, Queen Mary and Westfield College University of London, London, UK.

Hernández-Montes, E., Fernández-Ruiz, M.A., Aschheim, M. and Gil-Martín, L.M. (2017) 'Structural knowledge within the 6th century AD arch of Taq-iKisra', *International Journal of Architectural Heritage*, Vol. 11, No. 6, pp.891–900.

Illampas, R., Charmpis, D.C. and Ioannou, I. (2014) 'Finite element simulation of the structural response of adobe masonry buildings subjected to lateral loading', in *Proceedings 9th International Conference Structural Analysis Historical Constructions*, Mexico City, Mexico. pp.1–12.

Invernizzi, A. and Lippolis, C. (2008) *Nisa Partica – Ricerche nel complesso monumentale arsacide 1990-2006*, Monografie di Mesopotamia, Le Lettere, Firenze.

Jankowiak, T. and Lodygowski, T. (2005) 'Identification of parameters of concrete damage plasticity constitutive model', *Foundations of Civil and Environmental Engineering*, Vol. 6, pp.53–69.

Karanikoloudis, G. and Lourenço, P.B. (2018) 'Structural assessment and seismic vulnerability of earthen historic structures. Application of sophisticated numerical and simple analytical models', *Engineering Structures*, April, Vol. 160, pp.488–509.

Lourenço, P. and Pereira, J.M. (2018) *Seismic Retrofitting Project: Recommendations for Advanced Modeling of Historic Earthen Sites*, The Getty Conservation Institute TecMinho – University of Minho, Los Angeles Guimarães, Portugal.

Maheri, M.R. (2005) 'Performance of building roofs in the 2003 Bam, Iran, earthquake', *Earthquake Spectra*, Vol. 21, Suppl. 1, pp.411–424.

Martins, T. and Varum, H. (2006) 'Adobe's mechanical characterization in ancient constructions: the case of Aveiro's region', *Materials Science Forum*, December, Vols. 514–516, pp.1571–1575.

Masturzo, N. (2008) 'Nisa Partica: Ricerche nel complesso monumentale arsacide 1990-2006', in Invernizzi, A. and Lippolis, C. (Eds.): No. 9, *Monografie di Mesopotamia*, pp.43–65, Le Lettere, Firenze.

Mecca, S. and Dipasquale, L. (Eds.) (2009) *Earthen Domes et Habitats: Villages of Northern Syria*, Edizioni ETS, Pisa, Italy.

Miccoli, L., Garofano, A., Fontana, P. and Müller, U. (2015) 'Experimental testing and finite element modelling of earth block masonry', *Engineering Structures*, December, Vol. 104, pp.80–94.

Morel, J-C., Pkla, A. and Walker, P. (2007) 'Compressive strength testing of compressed earth blocks', *Construction and Building Materials*, Vol. 21, No. 2, pp.303–309.

Morris, J., Morris, J. and Blier, S.P. (2004) *Butabu: Adobe Architecture of West Africa*, Princeton Architectural Press, New York.

Parisi, F., Asprone, D., Fenu, L. and Prota, A. (2015) 'Experimental characterization of Italian composite adobe bricks reinforced with straw fibers', *Composite Structures*, April, Vol. 122, pp.300–307.

Parisi, F., Balestrieri, C. and Varum, H. (2019) 'Nonlinear finite element model for traditional adobe masonry', *Construction and Building Materials*, October, Vol. 223, pp.450–462.

Pereira, H. (2008) *Caracterization of the Structural Behaviour of Adobe Constructions*, in Portuguese, PhD dissertation, Department of Civil Engineering, Aveiro University, Aveiro, Portugal.

Piattoni, Q., Quagliarini, E. and Lenci, S. (2011) 'Experimental analysis and modelling of the mechanical behaviour of earthen bricks', *Construction and Building Materials*, Vol. 25, No. 4, pp.2067–2075.

Pope, A.U. (1930) *An Introduction to Persian Art Since the Seventh Century A.D.*, P. Davies, London.

Popovics, S. (1973) 'A numerical approach to the complete stress-strain curve of concrete', *Cement and Concrete Research*, Vol. 3, No. 5, pp.583–599.

Resta, M., Fiore, A. and Monaco, P. (2013) 'Non-linear finite element analysis of masonry towers by adopting the damage plasticity constitutive model', *Advances in Structural Engineering*, Vol. 16, No. 5, pp.791–803.

Rivera Torres, J.C. (2012) 'El adobe y otros materiales de sistemas constructivos en tierra cruda: caracterización con fines estructurales', *Apuntes: Revista de Estudios sobre Patrimonio Cultural – Journal of Cultural Heritage Studies*, Vol. 25, No. 2, pp.164–181.

Rovero, L. and Tonietti, U. (2012) 'Structural behaviour of earthen corbelled domes in the Aleppo's region', *Materials and Structures*, Vol. 45, No. 1, pp.171–184.

Silva, A., Oliveira, I., Silva, V., Mirão, J. and Faria, P. (2020) 'Vernacular Caramel's adobe masonry dwellings – material characterization', *International Journal of Architectural Heritage*, pp.1–18., in press, https://doi.org/10.1080/15583058.2020.1751343.

Silveira, D., Varum, H. and Costa, A. (2013) 'Influence of the testing procedures in the mechanical characterization of adobe bricks', *Construction and Building Materials*, March, Vol. 40, pp.719–728.

Silveira, D., Varum, H., Costa, A., Martins, T., Pereira, H. and Almeida, J. (2012) 'Mechanical properties of adobe bricks in ancient constructions', *Construction and Building Materials*, Vol. 28, No. 1, pp.36–44.

Simulia, D.S. (2018) *User's Manual*, Abaqus, Provid RI, USA DS SIMULIA Corp.

Tarque, N., Camata, G., Spacone, E., Blondet, M. and Varum, H. (2012) 'The use of continuum models for analyzing adobe structures', *WCEE*, Vol. 15, pp.2–5.

Tolles, E.L. (1996) *Survey of Damage to Historic Adobe Buildings after the January 1994 Northridge Earthquake*, GCI Scientific Program, Getty Conservation Institute, Los Angeles, CA.

Tolles, E.L., Kimbro, E.E., Webster, F.A., Ginell, W.S. et al. (2000) *Seismic Stabilization of Historic Adobe Structures: Final Report of the Getty Seismic Adobe Project*, Getty Conservation Institute, Los Angeles CA.

Tolstov, S. (2002) *Kul' turnye cennosti meždunarodnyj eždegonik*, Evrovpejskij Dom, Sankt Peterburg.

Torrealva, D., Vicente, E., Michiels, T. et al. (2018) *Seismic Retrofitting Project – Testing of Materials and Building Components of Historic Abobe Buildings in Peru*, The Getty Conservation Institute, Los Angeles, CA.

Varum, H., Costa, A., Fonseca J. and Furtado, A. (2015) 'Behaviour characterization and rehabilitation of adobe masonry', *Procedia Engineering*, Vol. 114, pp.714–721.

Varum, H., Figueiredo A., Costa, A., Silveira, D. and Carvalho, J. (2012) 'Characterization and strengthening of adobe constructions', in *Proceedings International Conference on Rehabilitation of Ancient Masonry Structures – CIRea2012*, in Portuguese, Lisbon, Portugal, pp.39–46.

Wosatko, A., Winnicki, A., Polak, M.A. and Pamin, J. (2019) 'Role of dilatancy angle in plasticity-based models of concrete', *Archives of Civil and Mechanical Engineering*, Vol. 19, No. 4, pp.1268–1283.

Wu, F., Li, G., Li, H-N. and Jia, J-Q. (2012) 'Strength and stress-strain characteristics of traditional adobe block and masonry', *Materials and Structures*, Vol. 46, No. 9, pp.1449–1457.

Zanazzi, E., Coïsson, E., Ferretti, D. and Lorenzelli, A. (2019) 'Masonry spires: 3D models to understand their seismic vulnerability', *Key Engineering Materials*, Vol. 817, pp.317–324.